The Journal of Immunology

Gp130-Dependent Astrocytic Survival Is Critical for the Control of Autoimmune Central Nervous System Inflammation

Fahad Haroon, Katrin Drögemüller, Ulrike Händel, Anna Brunn, Dirk Reinhold, Gopala Nishanth, Werner Mueller, Christian Trautwein, Matthias Ernst, Martina Deckert and Dirk Schlüter

J Immunol 2011; 186:6521-6531; Prepublished online 22 April 2011;
doi: 10.4049/jimmunol.1001135
http://www.jimmunol.org/content/186/11/6521

The Journal of Immunology is published twice each month by
The American Association of Immunologists, Inc.,
1451 Rockville Pike, Suite 650, Rockville, MD 20852

Print ISSN: 0022-1767 Online ISSN: 1550-6606.

Gp130-Dependent Astrocytic Survival Is Critical for the Control of Autoimmune Central Nervous System Inflammation

Fahad Haroon,* Katrin Drögemüller,* Ulrike Händel,* Anna Brunn,† Dirk Reinhold,‡ Gopala Nishanth,* Werner Mueller,§ Christian Trautwein,¶ Matthias Ernst,‖ Martina Deckert,† and Dirk Schlüter*

Astrocytes are activated in experimental autoimmune encephalomyelitis (EAE) and have been suggested to either aggravate or ameliorate EAE. However, the mechanisms leading to an adverse or protective effect of astrocytes on the course of EAE are incompletely understood. To gain insight into the astrocyte-specific function of gp130 in EAE, we immunized mice lacking cell surface expression of gp130, the signal-transducing receptor for cytokines of the IL-6 family, with myelin oligodendrocyte glycoprotein$_{35–55}$ peptide. These glial fibrillary acid protein (GFAP)-Cre gp130$^{fl/fl}$ mice developed clinically a significantly more severe EAE than control mice and succumbed to chronic EAE. Loss of astrocytic gp130 expression resulted in apoptosis of astrocytes in inflammatory lesions of GFAP-Cre gp130$^{fl/fl}$ mice, whereas gp130$^{fl/fl}$ control mice developed astrogliosis. Astrocyte loss of GFAP-Cre gp130$^{fl/fl}$ mice was paralleled by significantly larger areas of demyelination and significantly increased numbers of CD4 T cells in the CNS. Additionally, loss of astrocytes in GFAP-Cre gp130$^{fl/fl}$ mice resulted in a reduction of CNS regulatory Foxp3$^+$ CD4 T cells and an increase of IL-17–, IFN-γ–, and TNF-producing CD4 as well as IFN-γ– and TNF-producing CD8 T cells, illustrating that astrocytes regulate the phenotypic composition of T cells. An analysis of mice deficient in either astrocytic gp130– Src homology region 2 domain-containing phosphatase 2/Ras/ERK or gp130–STAT1/3 signaling revealed that prevention of astrocyte apoptosis, restriction of demyelination, and T cell infiltration were dependent on the astrocytic gp130–Src homology region 2 domain-containing phosphatase 2/Ras/ERK, but not on the gp130–STAT1/3 pathway, further demonstrating that gp130-dependent astrocyte activation is crucial to ameliorate EAE. *The Journal of Immunology*, **2011, 186: 6521–6531.**

Autoimmune diseases of the CNS are characterized by leukocyte recruitment to the CNS and activation of resident cells, including astrocytes. In these disorders, pathogenetically important leukocyte populations have been identified and characterized, whereas the selective in vivo function of CNS resident cells is poorly defined.

Murine myelin oligodendrocyte glycoprotein (MOG)$_{35–55}$-induced experimental autoimmune encephalomyelitis (EAE) is a T cell-mediated demyelinating disease characterized by a prominent activation of astrocytes and the development of astrogliosis in the vicinity of demyelinated lesions (1). Experimental evidence suggests that early astrocyte activation can promote EAE. NF-κB–driven astrocyte activation contributes to a more severe course of EAE characterized by an increased expression of proinflammatory cytokines and chemokines as well as increased demyelination (2, 3). This astrocytic NF-κB activation is critically regulated by IL-17–mediated activation of Act1; in the absence of astrocytic Act1 signaling, mice are largely protected from EAE and CD4 T cell infiltration to the spinal cord (4, 5). At later stages of EAE, reduced uptake of toxic molecules, inhibition of remyelination by scar formation, and blocking of axonal regeneration may contribute to disease progression (6, 7, reviewed in Ref. 8). However, astrocytes can also confer protection against EAE by reducing leukocyte infiltration into the CNS, induction of T cell apoptosis, production of immunosuppressive cytokines including IL-27, induction of regulatory T cells, inhibition of autoreactive T cell activation as well as enhancing myelin repair, and neuroprotection (8–14). These complex and in part opposing effects of astrocytes on EAE indicate that astrocyte function may be influenced by various factors, including the time point of disease, the local inflammatory milieu, regional differences of astrocyte function, or even astrocyte subtypes (reviewed in Refs. 8, 14).

The gp130 receptor is an essentially ubiquitous signal transducer for members of the IL-6 cytokine family, which includes IL-6, IL-11, IL-27, leukemia inhibitory factor (LIF), oncostatin M (OSM), ciliary neurotrophic factor (CNTF), B cell-stimulating factor (BSF)3, and cardiotrophin (CT)-1 (15). Gp130-deficient mice die perinatally and suffer from a more severe phenotype than mice deficient for individual gp130 ligands (for review, see 15). This

*Institut für Medizinische Mikrobiologie, Otto-von-Guericke-Universität Magdeburg, 39120 Magdeburg, Germany; †Abteilung für Neuropathologie, Universität zu Köln, 50937 Köln, Germany; ‡Institut für Molekulare und Klinische Immunologie, Otto-von-Guericke Universität Magdeburg, 39120 Magdeburg, Germany; §Faculty of Life Sciences, University of Manchester, Manchester M13 9PT, United Kingdom; ¶Medical Clinic III, Rheinisch-Westfälische Technische Hochschule-University Hospital Aachen, 52074 Aachen, Germany; and ‖Ludwig Institute for Cancer Research, Royal Melbourne Hospital, Victoria 3050, Australia

Received for publication April 7, 2010. Accepted for publication March 21, 2011.

This work was supported by Grant Schl 392/7-1 from Deutsche Forschungsgemeinschaft.

Address correspondence and reprint requests to Dr. Dirk Schlüter, Institut für Medizinische Mikrobiologie, OvG Universität Magdeburg, Leipzigerstrasse 44, 39120 Magdeburg, Germany. E-mail address: dirk.schlueter@medizin.uni-magdeburg.de

The online version of this article contains supplemental material.

Abbreviations used in this article: 7-AAD, 7-aminoactinomycin D; BSF, B cell-stimulating factor; CNTF, ciliary neurotrophic factor; CT, cardiotrophin; EAE, experimental autoimmune encephalomyelitis; GFAP, glial fibrillary acid protein; HPRT, hypoxanthine phosphoribosyltransferase; iNOS, inducible NO synthase; LIF, leukemia inhibitory factor; MOG, myelin oligodendrocyte glycoprotein; OSM, oncostatin M; p.i., postimmunization; SHP2, Src homology region 2 domain-containing phosphatase 2; WT, wild-type.

also explains why the function of gp130 is still unknown in cerebral autoimmune disorders, whereas the function of gp130 ligands and coreceptors has been partially characterized. In EAE, IL-27Rα, which forms a signaling complex in combination with gp130, plays a crucially protective role by inhibiting immunopathology mediated by IL-17–producing CD4 T cells (16). In contrast, mice lacking IL-6 developed impaired autoimmune T cell responses after immunization with MOG Ag, resulting in an increased resistance to EAE (17). Further studies with CNTF$^{-/-}$ and LIFβR$^{-/-}$ mice have shown that gp130-dependent signal transduction is important for limiting EAE by enhancing oligodendrocyte survival (18, 19). Collectively, these data indirectly indicate a regulatory role for gp130 in autoimmune CNS disorders, but it is unknown whether responsiveness of astrocytes to gp130-stimulating cytokines impacts on the disease.

Stimulation of gp130 results in the phosphorylation of a single membrane-proximal Y residue in gp130 (Y_{757} in mouse gp130), which induces the recruitment of the SH2 domain-containing cytoplasmic protein tyrosine phosphatase Src homology region 2 domain-containing phosphatase 2 (SHP2), its subsequent tyrosine phosphorylation, and activation of the Ras-ERK1/2 MAPK cascade (20). In contrast, binding of STAT1 and STAT3 proteins to the membrane-distal phosphotyrosine residues within gp130 (20) results in their tyrosine phosphorylation, homo- and/or heterodimerization, nuclear translocation, and transcriptional activation of target genes. Importantly, the gp130-dependent Ras and STAT1/3 pathways negatively control each other (21). To analyze the specific function of these two signaling pathways, mice lacking either gp130-STAT or gp130-Ras signaling have been generated (21, 22).

To characterize the in vivo function of astrocytes in autoimmune CNS disorders, we induced EAE in mice that lack gp130–, gp130-SHP2/Ras/ERK–, or gp130-STAT1/3–dependent signaling specifically in astrocytes. These experiments revealed the following: 1) astrocytic gp130 expression was crucial for survival of astrocytes and development of astrogliosis in EAE; 2) astrocyte loss exacerbated EAE characterized by significantly larger areas of demyelination and proinflammatory T cell response; and 3) the astrocytic gp130-SHP2/Ras/ERK pathway protected astrocytes from apoptosis and ameliorated EAE.

Materials and Methods

Mice

C57BL/6 human glial fibrillary acid protein (GFAP)-Cre transgenic mice (23) were bred with C57BL/6 gp130$^{fl/fl}$ (24) mice to generate GFAP-Cre$^{+/-}$ gp130$^{fl/fl}$ mice. To obtain Synapsin I-Cre gp130$^{fl/fl}$ mice, C57BL/6 Syn-Cre (25) and gp130$^{fl/fl}$ mice were bred. The colonies were maintained by breeding of GFAP-Cre$^{+/-}$ gp130$^{fl/fl}$ with GFAP-Cre$^{-/-}$ gp130$^{fl/fl}$ mice, and Synapsin-Cre$^{+/-}$ gp130$^{fl/fl}$ with Synapsin-Cre$^{-/-}$ gp130$^{fl/fl}$ mice, respectively. GFAP-Cre gp130$^{fl/Y757F}$ and GFAP-Cre gp130$^{fl/\Delta STAT}$ were generated by breeding of GFAP-Cre gp130$^{fl/fl}$ mice with either C57BL/6$^{wt/Y757F}$ or C57BL/6$^{wt/\Delta STAT}$ (21) mice. The colony was maintained by breeding of GFAP-Cre gp130 gp130$^{fl/Y757F}$ and GFAP-Cre gp130$^{fl/\Delta STAT}$ with gp130$^{fl/fl}$ mice, respectively. The genotype of offsprings was determined by PCR of tail DNA using primers for GFAP-Cre, Synapsin-Cre, gp130$^{fl/fl}$, gp130 ^{Y757F}, and gp130$^{\Delta STAT}$, respectively. C57BL/6 wild-type (WT) mice were obtained from Harlan (Borchen, Germany). Animal care and experimental procedures were performed according to European regulations and approved by state authorities (Landesverwaltungsamt Halle, Germany).

Induction and clinical evaluation of EAE

$MOG_{35–55}$ (MEVGWYRSPFSRVVHLYRNGK) was purchased from JPT (Berlin, Germany). EAE was induced in 8- to 12-wk-old mice by s.c. immunization with 200 μg $MOG_{35–55}$ in CFA (Sigma-Aldrich, Taufkirchen, Germany) containing 800 μg killed *Mycobacterium tuberculosis* (Sigma-Aldrich). In addition, 200 ng pertussis toxin (Sigma-Aldrich), dissolved in 200 μl PBS, was injected i.p. at the day of immunization and again 2 d thereafter. In indicated experiments, mice were immunized for a second time with 200 μg $MOG_{35–55}$ peptide in CFA (Sigma-Aldrich) containing 800 μg killed *M. tuberculosis* (Sigma-Aldrich) 7 d after primary immunization. Mice were monitored daily for clinical signs of EAE and graded on a scale of increasing severity from 0 to 5, according to a previously published grading scale (26) and detailed in Supplemental Table I. Daily clinical scores were calculated as the average of all individual disease scores within each group.

Histology

For immunohistochemistry on frozen sections, mice were perfused intracardially with 0.9% NaCl in methoxyflurane anesthesia. Brains were shock frozen, and immunohistochemistry for CD45, CD4, and CD8 was performed, as described before (27). For histology on paraffin sections, anesthetized mice were perfused with 4% paraformaldehyde in PBS; brains and spinal cords were processed and stained with hemalum and eosin, cresyl violet, luxol fast blue, and periodic acid Schiff stain, and also used for immunohistochemical demonstration of GFAP, neurofilament, Mac3, and CD3. CD3 (Serotec, Düsseldorf, Germany), S100 protein (DakoCytomation, Hamburg, Germany), and GFAP were demonstrated in an ABC protocol, as described (27).

Stereology

To quantify numbers of astrocytes and areas of demyelination in the spinal cord, stereology was applied using a computerized stereology system (Cast Software, Olympus, Germany). Serial cross sections (4 μm) of the entire spinal cord, that is, cervical, thoracic, and lumbar level, were cut. Every third section was either stained with rat anti-mouse GFAP, slightly counterstained with hemalum, or stained with luxol fast blue and cresyl violet, respectively. The volume of the entire spinal cord and the volume of the white matter, respectively, were determined according to Cavalieri's method (28) by estimating the area of every third section with the computerized system and multiplication with the distance to the next cross section evaluated, that is, 12 μm. Nuclei of GFAP-labeled astrocytes were counted. To avoid repetitive counting of astrocytes in adjacent cross sections, every third section was evaluated. Numbers of astrocytes/mm^3 were compared between the experimental groups. To compare areas of demyelination, the area of gray matter plus demyelinated white matter was related to the total area of the respective cross section.

Isolation of cerebral leukocytes and flow cytometry

Leukocytes were isolated from brain and spinal cord and stained for CD4$^+$ T cells, CD8$^+$ T cells, and CD45^{high} inflammatory leukocytes, as described before (29). For intracellular cytokine staining, isolated leukocytes were incubated with 50 ng/ml PMA, 500 ng/ml ionomycine, and Golgi-Plug (1 μl/ml) containing brefeldin A in MEM-α at 37°C for 4 h. Thereafter, cells were stained with CD4-FITC and CD8-allophycocyanin; fixed and permeabilized with Cytofix/Cytoperm (BD Biosciences, Heidelberg, Germany); and stained with rat anti-mouse IL-17–PE, TNF-PE, or IFN-γ–PE (BD Biosciences). Controls included staining with isotype-matched control Abs. For the detection of regulatory and activated CD4 T cells, isolated leukocytes were incubated with CD25-FITC and CD4-allophycocyanin, followed by a Foxp3-PE staining kit, as recommended by the manufacturer (NatuTec/eBiosciences, Frankfurt, Germany). Apoptotic and dead CD4 T cells were detected by staining with annexin V, 7-aminoactinomycin D (7-AAD), and CD4-allophycocyanin, or active caspase-3–PE and CD4-allophycocyanin. All Abs and reagents were obtained from BD Biosciences. Controls included staining with isotype-matched control Abs. Flow cytometry was performed on a FACScan (BD Biosciences), and the data were analyzed with WinMDI or CellQuest software.

Quantitative RT-PCR

For RT-PCR, mRNA was isolated from the spinal cord of nonimmunized and $MOG_{35–55}$-immunized mice (RNeasy kit; Qiagen). mRNA was transcribed into cDNA by use of a SuperScript reverse-transcriptase kit with oligo(dT) primers (Invitrogen). Quantitative PCR for the gp130 ligands IL-6, LIF, CNTF, OSM, CT-1, BSF3, IL-11, and IL-27 was performed with cDNA derived from C57BL/6 WT mice. The ratio between the respective cytokine and hypoxanthine phosphoribosyltransferase (HPRT) was calculated per mouse, and data are presented as the increase over nonimmunized mice. Quantitative RT-PCR for IL-17, IFN-γ, IL-23, inducible NO synthase (iNOS), TNF, TGF-β2, IL-27, and HPRT was performed with cDNA from GFAP-Cre gp130$^{fl/fl}$ and gp130$^{fl/fl}$ mice with the GeneAmp 5700 sequence detection system (Applied Biosystems, Foster City, CA). Quantitation was performed with the sequence detector software SDS 2.1 (Applied Biosystems), according to the ΔΔ cycle threshold method (30) with HPRT as housekeeping gene. Data are expressed as increase of mRNA expression in

immunized mice over nonimmunized controls of the respective mouse strain. All primers and probes were obtained from Applied Biosystems.

Statistics

Demyelinated areas and astrocyte numbers were evaluated on serial 4-μm cross sections of the spinal cord, which were either stained with luxol fast blue and cresyl violet or anti-GFAP and hemalum, respectively. Every third section was evaluated. For statistical evaluation of the number of $GFAP^+$ astrocytes on GFAP-immunostained sections, at least 50 high power fields (final original magnification ×400), randomly selected from all areas of various regions of the spinal cord, were analyzed per section in three animals per group. Differences were analyzed with the nonparametric Mann-Whitney rank sum test. To test for statistical differences in the survival rate, clinical scores, and cell numbers, the two-tailed Student *t* test was used. The *p* values <0.05 were accepted as significant. All experiments were performed at least twice.

Results

Upregulation of gp130 ligands in EAE

Because the gp130 receptor is essential for signal transduction of molecules of the IL-6 cytokine family, we analyzed whether expression of single or multiple members of this family is regulated in the spinal cord of mice suffering from EAE. At 14 d post-immunization (p.i.), expression of IL-6, LIF, OSM, and IL-27 was markedly upregulated, whereas expression of CNTF, CT-1, BSF3, and IL-11 was unaltered (Fig. 1). At this stage of EAE, mice had a mean clinical score of 2.2, and up to 25 d p.i. clinical scores declined to 0.9. In parallel to regressing disease activity, mRNA levels of IL-6, LIF, OSM, and IL-27 declined, although levels of LIF and OSM were still increased as compared with nonimmunized mice (Fig. 1).

Aggravated EAE of GFAP-Cre gp130$^{fl/fl}$

To study the functional role of astrocytic gp130 expression, we used GFAP-Cre $gp130^{fl/fl}$ mice, which lack gp130 cell surface expression on astrocytes (31). We have previously shown that in this mutant macroscopically and histopathologically brain architecture is normal, including a regular number and morphology of $GFAP^+$ astrocytes (31).

Clinically, GFAP-Cre $gp130^{fl/fl}$ mice developed a significantly more severe EAE as compared with $gp130^{fl/fl}$ control mice upon immunization with $MOG_{35–55}$ (Fig. 2*A*; for definition of clinical score, see Supplemental Table 1). In addition, GFAP-Cre $gp130^{fl/fl}$ mice did not recover from disease and 50–84% died of EAE. In contrast, only 10–15% of controls died of EAE.

To analyze whether differences in clinical disease activity between the two groups were influenced by the strength of immunization, mice were immunized for a second time with $MOG_{35–55}$ peptide 7 d after primary immunization. Double immunization resulted in a higher maximal clinical score without subsequent decline in $gp130^{fl/fl}$ mice as compared with single-immunized mice (Fig. 2*B*). In GFAP-Cre $gp130^{fl/fl}$ mice, double immunization induced a very rapid progression of clinical symptoms, and peak scores developed within 5 d after disease onset without regression thereafter (Fig. 2*B*). Because single immunization was sufficient to induce maximal disease scores in GFAP-Cre $gp130^{fl/fl}$ mice, we used the single-immunization protocol in further experiments.

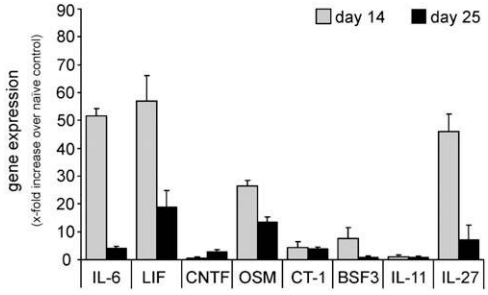

FIGURE 1. Upregulation of IL-6 family cytokine mRNA in EAE. mRNA transcription of IL-6 family cytokine members in the spinal cord was evaluated by quantitative RT-PCR in nonimmunized and $MOG_{35–55}$-immunized C57BL/6 mice at 14 and 25 d p.i. Data are expressed as increase of the respective cytokine mRNA of immunized over nonimmunized mice normalized to HPRT expression. Three mice per group were analyzed. Data represent the mean ± SEM. Data from one of two independent experiments are shown.

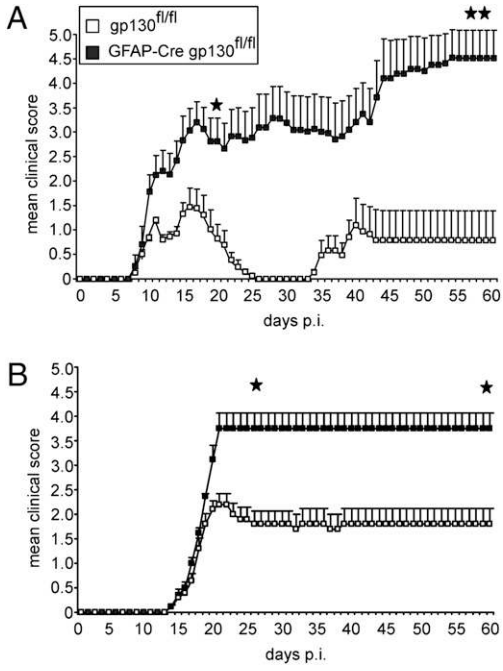

FIGURE 2. Increased clinical EAE severity in GFAP-Cre $gp130^{fl/fl}$ mice. *A* and *B*, The clinical scores of GFAP-Cre $gp130^{fl/fl}$ and $gp130^{fl/fl}$ mice were monitored daily up to 60 d after single (*A*) or double (*B*) immunization with $MOG_{35–55}$ peptide. Data show the mean ± SEM. Eight to 10 (*A*) and six (*B*), respectively, mice per experimental group were analyzed. At 20 and 60 d p.i., clinical score and disease incidence were significantly increased in GFAP-Cre $gp130^{fl/fl}$ mice as compared with $gp130^{fl/fl}$ mice ($*p < 0.05$, $**p < 0.01$). Data from one of three (*A*) and one of two (*B*) independent experiments are shown.

Because GFAP-Cre–driven deletion of gp130 also results in lack of gp130 expression in ~10% of neurons (31), we also established mice with neuron-specific, Synapsin I-Cre–mediated deletion of gp130 (Supplemental Fig. 2*A–C*). It has been shown before that Synapsin I-Cre efficiently deletes genes in the vast majority of neurons in all regions of the CNS, including the spinal cord (25). Importantly, Synapsin I-Cre $gp130^{fl/fl}$ mice showed the same course of EAE as $gp130^{fl/fl}$ mice (Supplemental Fig. 2*D*), demonstrating that the absence of gp130 on astrocytes, but not on neurons, is responsible for aggravation of EAE in GFAP-Cre $gp130^{fl/fl}$ mice.

Astrocyte loss in GFAP-Cre gp130$^{fl/fl}$ mice with EAE

To study the impact of astrocyte-specific gp130 expression on EAE challenge, a detailed stereological analysis was performed. Numbers of astrocytes in the spinal cord of GFAP-Cre $gp130^{fl/fl}$

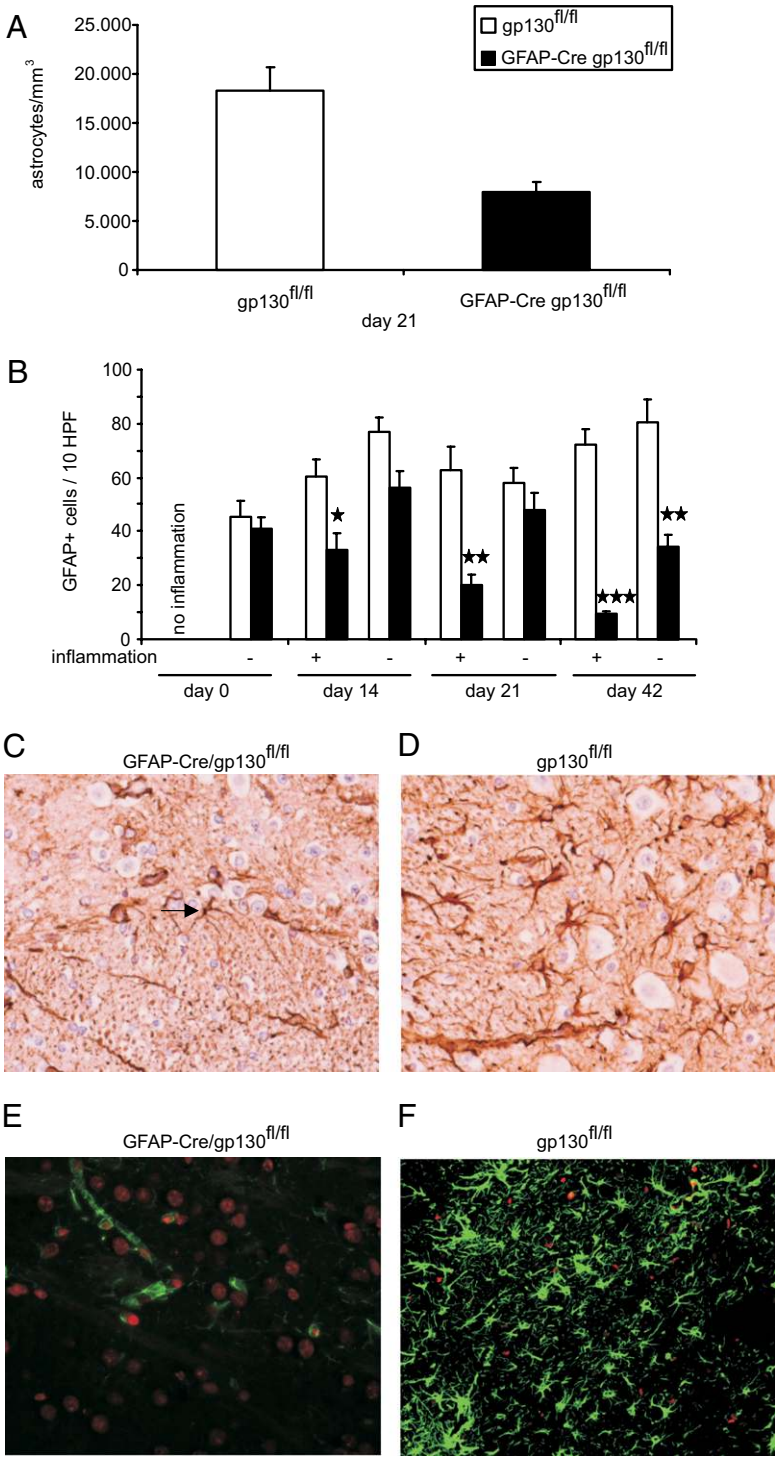

FIGURE 3. Reduced numbers of GFAP$^+$ astrocytes in EAE of GFAP-Cre gp130$^{fl/fl}$ mice. *A*, Numbers of spinal cord GFAP$^+$ astrocytes were quantitated by stereology in serial cross sections (4 μm) of the entire spinal cord. Data show the numbers of astrocytes per mm^3 ± SEM. Astrocyte numbers were significantly reduced in GFAP-Cre gp130$^{fl/fl}$ as compared with gp130$^{fl/fl}$ mice ($p < 0.03$). *B*, To determine astrocyte numbers in regions with or without inflammation, GFAP$^+$ cells were quantitated by a nonstereological method based on counting numbers of immunoreactive cells in at least 50 high power fields of anti-GFAP–stained sections of the spinal cord from $MOG_{35–55}$-immunized GFAP-Cre gp130$^{fl/fl}$ and gp130$^{fl/fl}$ mice. Three mice were analyzed per time point. The mean ± SEM is shown. *C*, Only low numbers of GFAP$^+$ astrocytes are present in the spinal cord of a GFAP-Cre gp130$^{fl/fl}$ mouse at 14 d p.i. Arrow points to an apoptotic GFAP$^+$ astrocyte. *D*, In contrast, strongly activated GFAP$^+$ astrocytes are present in a gp130$^{fl/fl}$ mouse. *C* and *D*, Anti-GFAP immunostaining, slight counterstaining with hemalum, original magnification ×200. *E* and *F*, Whereas many TUNEL$^+$ (red) apoptotic astrocytes with faint GFAP staining (green) are present in the spinal cord of a GFAP-Cre gp130$^{fl/fl}$ mouse, apoptotic astrocytes are rare in the spinal cord of a gp130$^{fl/fl}$ mouse at 14 d p.i. Reactive astrogliosis is only present in the gp130$^{fl/fl}$ mouse (*F*). Original magnification ×100. *A–F*, Data from one of two independent experiments are shown. *$p < 0.05$, **$p < 0.01$, ***$p < 0.005$.

mice were significantly reduced as compared with gp130$^{fl/fl}$ control animals (Fig. 3*A*). In GFAP-Cre gp130$^{fl/fl}$ mice, astrocyte loss was observed at all levels of the spinal cord, that is, the cervical, thoracic, and lumbar segment. In addition to this three-dimensional analysis of astrocyte numbers, standard immunohistochemistry showed a gradual loss of astrocytes within inflammatory and demyelinated lesions over time in GFAP-Cre gp130$^{fl/fl}$ mice (Fig. 3*B*). In contrast, the number of activated astrocytes increased in inflammatory lesions of control mice and was significantly increased in comparison with GFAP-Cre gp130$^{fl/fl}$ mice at all time points after $MOG_{35–55}$ immunization (Fig. 3*B*). Interestingly, astrocyte numbers of gp130$^{fl/fl}$ mice also increased in noninflamed regions of the spinal cord and were significantly higher as compared with GFAP-Cre gp130$^{fl/fl}$ mice at 42 d p.i. (Fig. 3*B*).

As early as 14 d p.i., the decline in astrocyte numbers in inflammatory lesions of GFAP-Cre gp130$^{fl/fl}$ mice was paralleled by the frequent appearance of astrocytes with crinkled processes and a condensed nucleus, indicating their apoptosis (Fig. 3*C*). Activated, hypertrophic GFAP$^+$ astrocytes were only rarely observed in the lesions of GFAP-Cre gp130$^{fl/fl}$ mice (Fig. 3*C*). These findings became more prominent with disease progression, and the inflammatory lesions of GFAP-Cre gp130$^{fl/fl}$ mice were nearly completely devoid of astrocytes at 42 d p.i. (data not shown). In contrast, activated astrocytes in inflammatory lesions of control

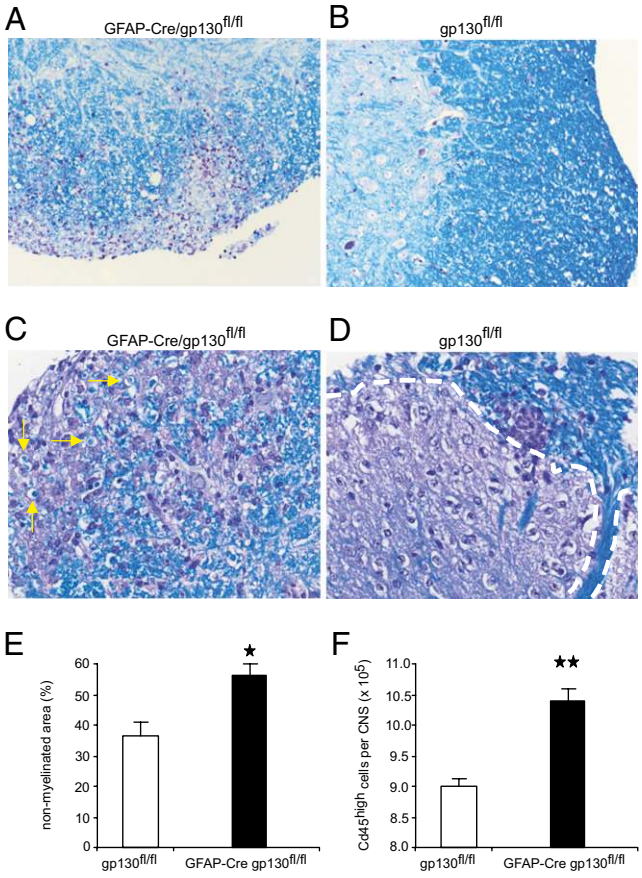

FIGURE 4. Increased demyelination and persistence of inflammatory infiltrates and T cells in EAE of GFAP-Cre gp130$^{fl/fl}$ mice. *A–D*, Inflammation and demyelination are more pronounced in the spinal cord of a GFAP-Cre gp130$^{fl/fl}$ mouse (*A*, *C*) as compared with a gp130$^{fl/fl}$ mouse (*B*, *D*) at 42 d p.i. Numerous myelophages are found in the white matter of the spinal cord of a GFAP-Cre gp130$^{fl/fl}$ mouse (arrows, *C*). In contrast, only a small inflammatory infiltrate is present in a gp130$^{fl/fl}$ mouse in the white matter at the border to the gray matter, and myelophages are absent (*D*, the border between gray and white matter is marked by a dashed white line). Cresyl violet and luxol fast blue staining, original magnification ×100 (*A*, *B*); H&E and luxol fast blue staining, original magnification ×200 (*C*, *D*). *E*, Stereology showed that the size of the demyelinated area in the spinal cord was significantly increased in GFAP-Cre gp130$^{fl/fl}$ mice at 20 d p.i. ($*p < 0.02$). *F*, At 20 d p.i., the number of inflammatory CD45^{high} leukocytes is significantly increased in the CNS of GFAP-Cre gp130$^{fl/fl}$ as compared with GFAP-Cre gp130$^{fl/fl}$ mice ($**p < 0.01$) as revealed by flow cytometry. Three mice (*E*) and six mice (*F*) per group were analyzed, and data represent the mean ± SEM. Data from one of two independent experiments are shown.

mice upregulated GFAP and were hypertrophic with long and extended cellular processes resulting in astrogliosis (Fig. 3*D*, 3*F*). Combined TUNEL and GFAP staining revealed that at all time points of EAE, astrocytes of GFAP-Cre gp130$^{fl/fl}$ mice underwent apoptosis. Most of the TUNEL$^+$ cells still exhibited a faint GFAP staining, which is compatible with a rapid degradation of this cytoskeletal protein (Fig. 3*E*). In contrast, only a few GFAP$^+$ astrocytes were TUNEL$^+$ in gp130$^{fl/fl}$ mice (Fig. 3*F*). These findings indicate that gp130 expression of astrocytes is important for the protection of astrocytes against apoptosis and results in the development of astrogliosis in EAE.

Increased pathology and persistence of inflammatory infiltrates in EAE of GFAP-Cre gp130$^{fl/fl}$ mice

A histopathological analysis of the impact of astrocytic loss on demyelination and the inflammatory response in EAE revealed that GFAP-Cre gp130$^{fl/fl}$ mice exhibited a remarkably more pronounced demyelination in the caudal brain stem and the spinal cord than control mice (Fig. 4*A*, 4*C*). The demyelinated area was significantly enlarged in GFAP-Cre gp130$^{fl/fl}$ mice as compared with control animals (Fig. 4*E*). Whereas inflammation and demyelination were largely confined to the dorsal columns of the spinal cord in gp130$^{fl/fl}$ mice, inflammatory demyelination also affected the lateral and anterior areas of the spinal cord and also extended into the gray matter of the spinal cord of GFAP-Cre gp130$^{fl/fl}$ mice (Fig. 4*A*). The more widespread inflammation and demyelination persisted in chronic EAE of GFAP-Cre gp130$^{fl/fl}$ mice, when gp130$^{fl/fl}$ mice had already clinically recovered (Fig. 4*B*, 4*D*). Flow cytometric quantification of inflammatory leukocytes confirmed that numbers of leukocytes were significantly increased in the CNS of GFAP-Cre gp130$^{fl/fl}$ as compared with gp130$^{fl/fl}$ mice (Fig. 4*F*).

Increased numbers of CD4 T cells were paralleled by a reduction of regulatory CD4 T cells and an increase of proinflammatory cytokine-producing T cells in GFAP-Cre gp130$^{fl/fl}$ mice

Because autoimmune T cells are crucial for EAE development, we studied the distribution of T cells at an early (14 d p.i.) and late stage (42 d p.i.) of EAE. CD3$^+$ T cell infiltrates were present in both GFAP-Cre gp130$^{fl/fl}$ and control mice at 14 d p.i. Up to 42 d p.i., however, they had persisted only in GFAP-Cre gp130$^{fl/fl}$ mice, whereas they had largely been resolved in gp130$^{fl/fl}$ mice (Fig. 5*A–D*).

At 17 d p.i., a flow cytometric analysis of T cells revealed that GFAP-Cre gp130$^{fl/fl}$ mice harbored 2-fold more CD4 T cells in the CNS than gp130$^{fl/fl}$ control animals (Fig. 5*E*), which already started to recover from an EAE. In contrast, numbers of CD8 T cells did not differ significantly between the two genotypes (Fig. 5*E*).

It has been suggested that astrocytes induce apoptosis of autoimmune CD4 T cells (32), which may explain the increased numbers of CD4 T cells in GFAP-Cre gp130$^{fl/fl}$ mice. However, only in two of four experiments was a reduced percentage of 7-AAD$^+$ CD4 T cells obvious in GFAP-Cre gp130$^{fl/fl}$ mice. In addition, the percentage of active caspase-3$^+$ CD4 T cells was not reduced in GFAP-Cre gp130$^{fl/fl}$ mice (3.3 versus 5.9% in gp130$^{fl/fl}$ and GFAP-Cre gp130$^{fl/fl}$ mice, respectively), as revealed by flow cytometry.

In addition, astrocyte apoptosis influenced the activation and the phenotypic composition of CD4 T cells in EAE. The percentage of both Foxp3$^+$ CD25$^-$ and Foxp3$^+$ CD25$^+$ regulatory CD4 T cells was reduced in GFAP-Cre gp130$^{fl/fl}$ mice, whereas the number of activated Foxp3$^-$ CD25$^+$ effector CD4 T cells was increased as compared with control mice (Fig. 5*F*).

These differences in the number of regulatory and activated CD4 T cells were paralleled by an increase of IL-17–, TNF-, and IFN-γ–producing CD4 as well as TNF- and IFN-γ–producing CD8 T cells in the CNS of GFAP-Cre gp130$^{fl/fl}$ mice as compared with control animals (Fig. 5*G*, 5*H*). The increase of CD4 T cells was 4-fold for IL-17 and 3-fold for both TNF and IFN-γ, respectively. Thus, the increase in the number of cytokine-producing CD4 T cells exceeded the 2-fold difference in the absolute number of CD4 T cells in the CNS of GFAP-Cre gp130$^{fl/fl}$ mice (Fig. 5*E*). Similar observations were obtained for CD8 T cells, as follows: there was a 2-fold increase for TNF- and a 4-fold increase in IFN-γ–producing CD8 T cells in GFAP-Cre gp130$^{fl/fl}$ mice, respectively, despite a lack of difference in the absolute number of CD8 T cells in both strains of mice (Fig. 5*E*). Thus, astrocyte loss was associated with an increase of disease-promoting T cells, whereas protective T cell populations declined.

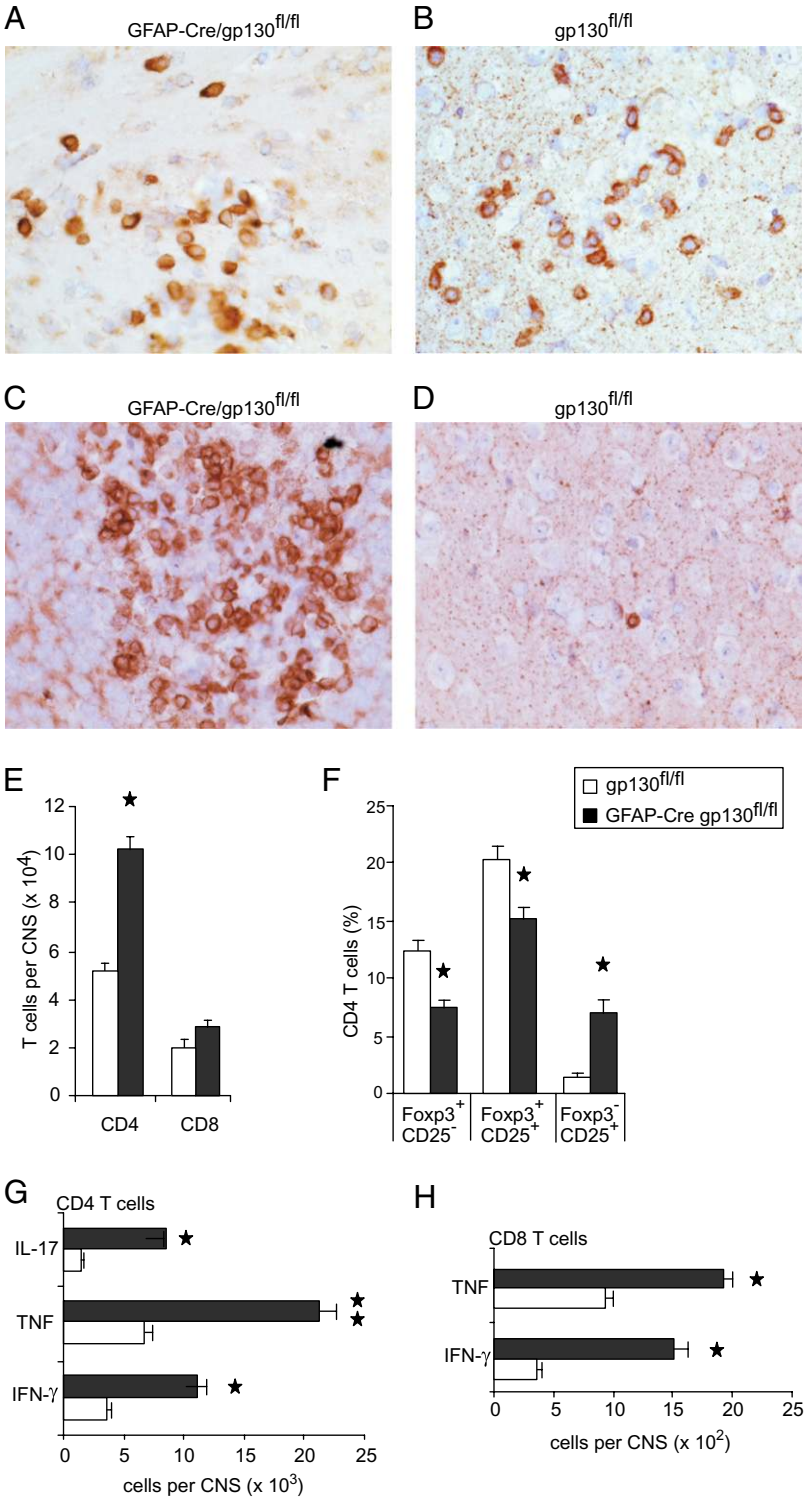

FIGURE 5. Persistence of CD4 T cells in GFAP-Cre gp130$^{fl/fl}$ mice is paralleled by a reduced number of regulatory CD4 T cells and increased numbers of IL-17–, IFN-γ–, and TNF-producing T cells. *A–D*, CD3$^+$ T cells are present in the spinal cord of a GFAP-Cre gp130$^{fl/fl}$ mouse at 14 d (*A*) and 42 d (*C*) p.i. In a gp130$^{fl/fl}$ mouse, CD3$^+$ T cells are present only at 14 d p.i. (*B*), but not at 42 d p.i. (*D*). Anti-CD3 immunostaining, slight counterstaining with hemalum; original magnification ×200. *E*, The number of CD4 T cells was significantly increased in the CNS of GFAP-Cre gp130$^{fl/fl}$ mice, whereas numbers of CD8 T cells did not differ. *F*, The percentage of Foxp3$^+$ and/or CD25$^+$ CD4 T cells was determined in the CNS by flow cytometry. *G* and *H*, The number of CD4 T cells producing IL-17, TNF, or IFN-γ (*G*) as well as the number of CD8 T cells producing TNF or IFN-γ (*H*) was determined by flow cytometry. *E–H*, Leukocytes were isolated from the CNS of GFAP-Cre gp130$^{fl/fl}$ and gp130$^{fl/fl}$ mice (six mice per group) and analyzed by flow cytometry at 17 d p.i. Data show the mean ± SEM. $*p < 0.05$, $**p < 0.01$. Data from one of two independent experiments are shown.

Increased IL-17, IFN-γ, IL-23, and iNOS mRNA production of GFAP-Cre gp130$^{fl/fl}$ mice

To gain further insight into the impact of astrocytes on cytokine production in EAE, cytokine mRNA transcription in the spinal cord was analyzed at an early (14 d p.i.) and a late time point (21 d p.i.) of EAE. At 14 d p.i., IL-17 mRNA was strongly upregulated in GFAP-Cre gp130$^{fl/fl}$ mice as compared with control animals (Fig. 6*A*). In contrast, IFN-γ, IL-23, TNF, iNOS, TGF-β2, and IL-27 mRNA did not differ between the two mouse strains at this time point (Fig. 6*B–G*). In addition to IL-17 mRNA, IFN-γ, IL-23, and iNOS mRNA were also strongly upregulated in GFAP-Cre gp130$^{fl/fl}$ mice at 21 d p.i. In contrast, TGF-β2 mRNA was increased in gp130$^{fl/fl}$ mice at this stage of EAE. No differences were observed for TNF and IL-27.

The gp130-SHP2/Ras/ERK, but not the gp130-STAT pathway ameliorates EAE, protects astrocytes from apoptosis, and reduces inflammatory infiltrates as well as demyelination

Ligand engagement of the gp130 receptor results in activation of the STAT1/3 and Ras/ERK pathway via specific tyrosine residues within the cytosolic portion of gp130. To evaluate the contribution

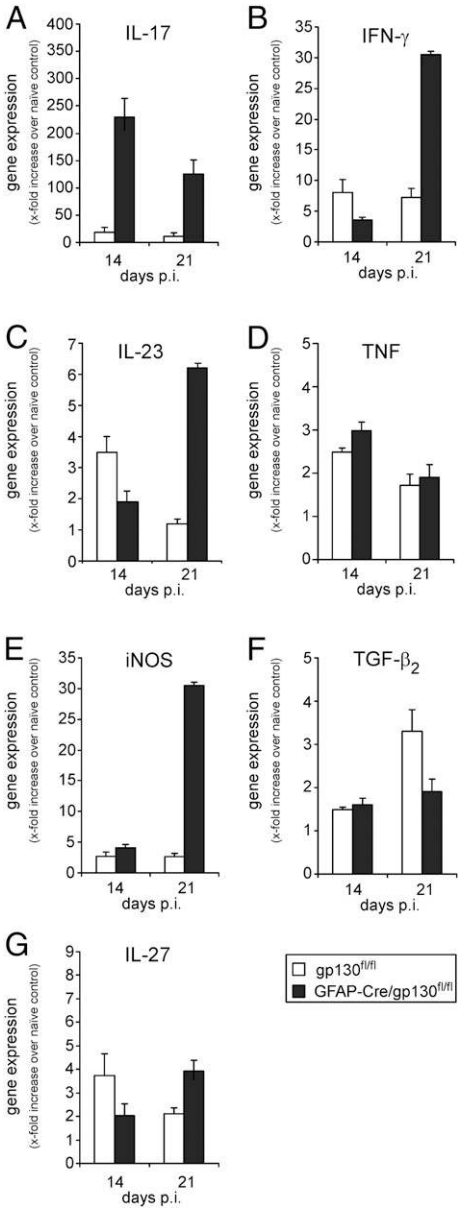

FIGURE 6. Increased IL-17, IFN-γ, IL-23, and iNOS mRNA transcription in EAE of GFAP-Cre gp130$^{fl/fl}$ mice. *A–F*, The mRNA expression of IL-17 (*A*), IFN-γ (*B*), IL-23 (*C*), TNF (*D*), iNOS (*E*), TGF-β2 (*F*), and IL-27 (*G*) was analyzed by quantitative RT-PCR from GFAP-Cre gp130$^{fl/fl}$ and gp130$^{fl/fl}$ mice at 14 and 21 d p.i. Spinal cords of three mice per group were analyzed, and data represent the mean ± SEM as relative increase over nonimmunized mice. One of two independent experiments is shown.

of the two pathways to ameliorate EAE, we used a breeding strategy to generate pseudo-tissue–specific mutant mice that harbored either one *gp130ΔSTAT* allele (resulting in the lack of STAT1/3 and excessive SHP2/Ras/ERK activation) or one *gp130Y757F* allele (resulting in the lack of SHP2/Ras/ERK and excessive STAT1/3 activation) (33). Accordingly, these mutant alleles become functionally dominant in astrocytes following interbreeding with GFAP-Cre gp130$^{fl/fl}$ mice and upon stimulation with IL-6 family ligands, in the resulting compound GFAP-Cre gp130$^{fl/\Delta STAT}$ and GFAP-Cre gp130$^{fl/Y757F}$ mice.

Upon immunization with $MOG_{35–55}$ peptide, GFAP-Cre gp130$^{fl/\Delta STAT}$ mice developed EAE clinically similar to gp130$^{fl/fl}$ control mice. In contrast, clinically GFAP-Cre gp130$^{fl/Y757F}$ mice suffered from much more severe symptoms than gp130-proficient control mice. Indeed, GFAP-Cre gp130$^{fl/Y757F}$ mice showed similar EAE scores to gp130-deficient GFAP-Cre gp130$^{fl/fl}$ mice (Fig. 7*A*). Histopathological analysis of GFAP-Cre gp130$^{fl/Y757F}$ mice revealed a strong and widespread loss of astrocytes in the spinal cord (Fig. 7*B*) similar to that observed in GFAP-Cre gp130$^{fl/fl}$ mice, whereas astrocytes of GFAP-Cre gp130$^{fl/\Delta STAT}$ mice were activated and hypertrophic despite a less severe disease activity (Fig. 7*C*). Loss of astrocytes in GFAP-Cre gp130$^{fl/\ Y757F}$ mice resulted in much more severe demyelination when compared with GFAP-Cre gp130$^{fl/\Delta STAT}$ mice, which showed only mild demyelination (Fig. 7*D*, 7*E*). Consistent with the different extent of demyelination, inflammatory infiltrates were much more prominent and widespread in GFAP-Cre gp130$^{fl/Y757F}$ mice than in GFAP-Cre gp130$^{fl/\Delta STAT}$ mice (Fig. 7*F*, 7*G*). Collectively, these observations suggest that the extent of gp130-mediated STAT activation in astrocytes, which occurs excessively in GFAP-Cre gp130$^{fl/Y757F}$ mice and is absent from GFAP-Cre gp130$^{fl/fl}$ mice, is not related to development of EAE. In contrast, the extent of EAE inversely correlates with the extent of gp130-mediated SHP2/Ras/ERK activation, which is absent in the highly disease-sensitive GFAP-Cre gp130$^{fl/Y757F}$ and GFAP-Cre gp130$^{fl/fl}$ strains, but present in gp130$^{fl/fl}$ controls and GFAP-Cre gp130$^{fl/\ \Delta STAT}$ mice. Therefore, we conclude that development of a protective astrogliosis is independent of gp130-mediated STAT signaling, but requires gp130-dependent SHP2/Ras/ERK signaling.

Discussion

The present in vivo experiments revealed that astrocyte-specific gp130 signaling is important to protect mice from EAE, because both single and double $MOG_{35–55}$-immunized mice lacking astrocyte-specific gp130 signaling developed a clinically significantly more severe EAE than control mice. The major protective function of astrocytic gp130 was to ensure astrocyte survival and to enable development of astrogliosis as important factors limiting autoimmune T cell reactions and demyelination in EAE. Such an important function of gp130 expression on astrocytes in EAE has not been observed in mice lacking individual gp130 ligands, including IL-6, LIF, and IL-27, respectively (16, 17, 34). However, all of these gp130 ligands were upregulated in EAE and, therefore, may compensate for each other in rescuing astrocytes from apoptosis under inflammatory conditions. This is in contrast to oligodendrocytes, which require CNTF and LIF to prevent their apoptosis in EAE (18, 19). The cell-type–specific importance of astrocytic gp130 is further stressed by the observation that mice lacking gp130 expression selectively in neurons developed the same course of EAE as gp130$^{fl/fl}$ control mice.

Gp130 expression of astrocytes was required to prevent apoptosis of astrocytes. In good agreement with an antiapoptotic function of gp130 (35), survival of astrocytes upon in vitro stimulation with TNF is gp130 dependent (31). Because in EAE a variety of cytokines including TNF is produced (36) (Figs. 5, 6), these molecules may also contribute to loss of GFAP-Cre gp130$^{fl/fl}$ astrocytes in vivo.

Astrocyte apoptosis rendered GFAP-Cre gp130$^{fl/fl}$ mice unable to mount astrogliosis in EAE. Recent studies in EAE using inducible astrocyte-deficient mice demonstrated that deletion of astrocytes in EAE prevents the development of astrogliosis, resulting in a more widespread inflammation and demyelination (10). Interestingly, we demonstrated previously that in *Toxoplasma* encephalitis gp130-dependent astrocyte survival and astrogliosis are important to restrict and contain inflammatory lesions (31). The concept of gp130-dependent astrogliosis as a CNS intrinsic and specific mechanism to restrict inflammatory

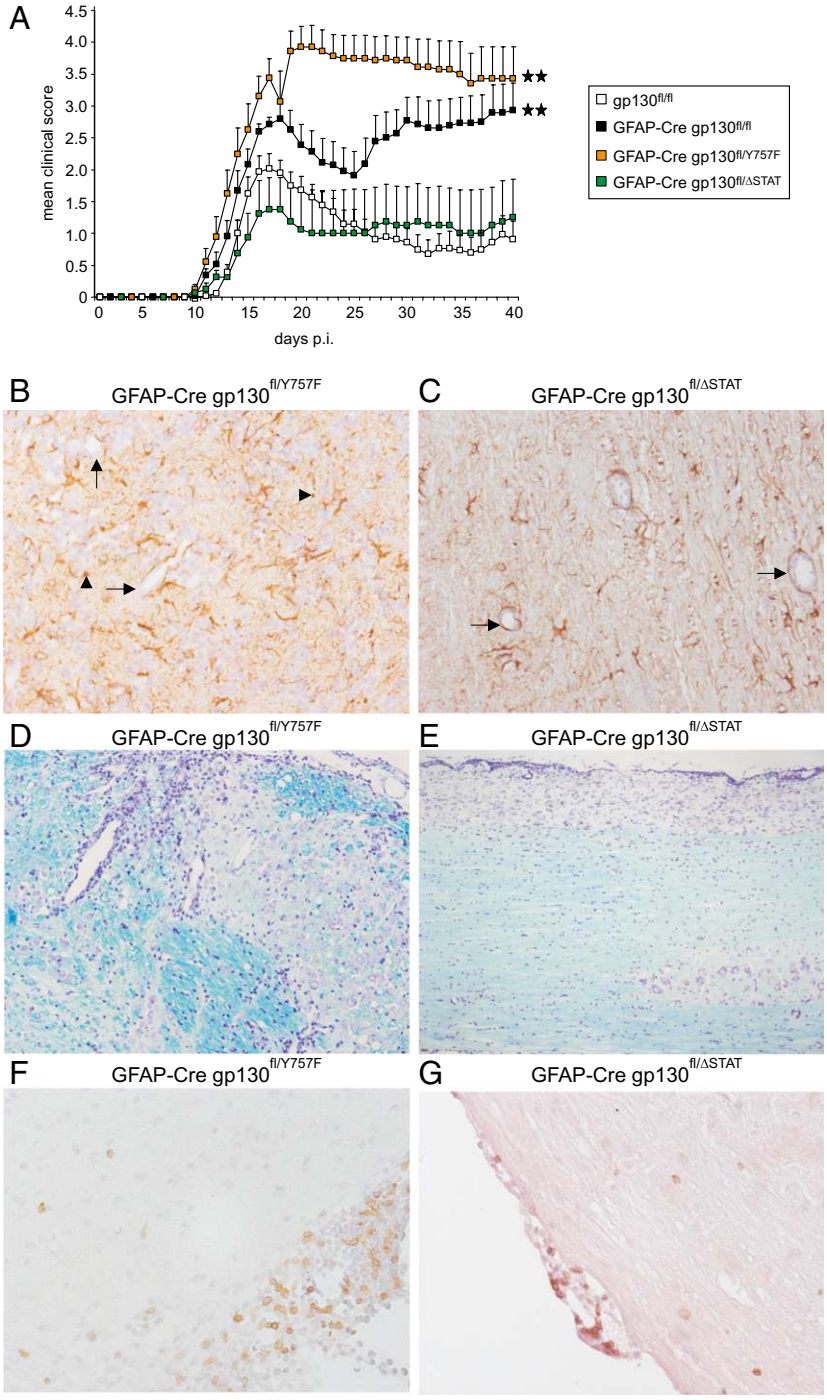

FIGURE 7. Aggravated EAE with widespread astrocyte loss, severe demyelination, and increased T cell infiltration in GFAP-Cre gp130$^{fl/Y757F}$ mice. *A*, The clinical score of GFAP-Cre gp130$^{fl/fl}$ and gp130$^{fl/fl}$ as well as GFAP-Cre gp130$^{fl/Y757F}$ and GFAP-Cre gp130$^{fl/\Delta STAT}$ mice was monitored daily up to 40 d p.i. with MOG_{35-55} peptide. Six to eight mice per experimental group were analyzed. Data show the mean ± SEM. The clinical score was significantly increased in GFAP-Cre gp130$^{fl/fl}$ and GFAP-Cre gp130$^{fl/Y757F}$ mice as compared with gp130$^{fl/fl}$ controls ($^{**}p < 0.01$). The clinical score of GFAP-Cre gp130$^{\Delta STAT}$ mice did not differ significantly from control mice. *B*, Partial loss of GFAP-expressing astrocytic processes perivascularly (arrows) and in a subleptomeningeal infiltrate in a GFAP-Cre gp130$^{fl/Y757F}$ mouse. Note the crinkled cellular processes and the condensed shrunken nuclei of astrocytes (arrowheads). *C*, Astrocytes of a GFAP-Cre gp130$^{fl/\Delta STAT}$ mouse were normally activated (arrows) in the spinal cord. *B* and *C*, Anti-GFAP immunostaining, slight counterstaining with hemalum, original magnification ×200. *D*, Loss of myelin and vacuolation in a subleptomeningeal infiltrate in a GFAP-Cre gp130$^{fl/Y757F}$ mouse. Note the intense perivascular and intraparenchymal inflammatory reaction (arrows). *E*, Regular myelination in the spinal cord with only slight leptomeningeal infiltrate in GFAP-Cre gp130$^{fl/\Delta STAT}$ mouse. *D* and *E*, Cresyl violet with luxol fast blue staining, original magnification ×100. *F*, CD3 T cells in a subleptomeningeal perivascular infiltrate and scattered throughout the brain parenchyma in a GFAP-Cre gp130$^{fl/Y757F}$ mouse. *G*, Single CD3 T cells in the leptomeninges and the spinal cord parenchyma of a GFAP-Cre gp130$^{fl/\Delta STAT}$ mouse. *F* and *G*, Anti-CD3 immunostaining, slight counterstaining with hemalum, original magnification ×200. *B–G*, Three mice were analyzed per experimental group at 17 d p.i. *A–G*, Representative data from one of two independent experiments are shown.

lesions is supported by the more widespread inflammation and demyelination in EAE of GFAP-Cre gp130$^{fl/fl}$ mice. Interestingly, patients suffering from acute multiple sclerosis are also characterized by astrocyte loss in the center of the demyelinated lesions and an astrogliosis surrounding these lesions (37).

Abrogation of gp130 signaling in astrocytes had a strong impact on the immune response in the CNS. The most striking observation was that loss of astrocytes in inflammatory lesions resulted in increased numbers of CD4 T cells in the CNS. Initially, GFAP-Cre gp130$^{fl/fl}$ mice recruited CD3 T cells to the CNS similar to control mice. This observation indicates that the early recruitment of T cells to the CNS was unimpaired in GFAP-Cre gp130$^{fl/fl}$ mice and that astrocytes were still able to contribute to T cell recruitment by their production of chemokines (38). However, once autoimmune inflammation was fully established, defective astrocytic gp130 signaling and rapid astrocyte apoptosis contributed to a failure to efficiently reduce CD4 T cell numbers in the CNS.

Previous experiments have demonstrated that the elimination of autoimmune T cells by apoptosis is important for EAE resolution (39, 40). Although it is at present unclear which cell types induce CD4 T cell apoptosis in EAE, astrocytes may be key inducers because of the following: 1) astrocytes are in intimate contact with apoptotic T cells and express Fas ligand (9); 2) autoreactive CD4 T cells are Fas$^+$ (41); and 3) Fas ligand$^+$ astrocytes induce apoptosis of MOG-specific T cells in vitro (42). However, flow cytometry showed only reduced numbers of 7-AAD$^+$, that is, late apoptotic or dead, CD4 T cells and failed to detect reduced active

caspase-3 expression in CNS CD4 T cells of GFAP-Cre gp130$^{fl/fl}$ mice in two of four experiments. These data indicate that gp130 expression of astrocytes is not crucial for the induction of CD4 T cell apoptosis, although they do not principally rule out the possibility that astrocytes may induce apoptosis of autoimmune CD4 T cells.

The increased number of CD4 T cells in the CNS might also be caused by an increased homing of these cells to the spinal cord of GFAP-Cre gp130$^{fl/fl}$ mice. Our observation of a strong reduction in the number of perivascular astrocytes in inflamed areas of the spinal cord of GFAP-Cre gp130$^{fl/fl}$ mice and the observation of Voskuhl et al. (10) that depletion of proliferating astrocytes in EAE results in an increased influx of inflammatory leukocytes into the spinal cord indicate that perivascular astrocytes restrict the recruitment of CD4 T cells to the CNS. Thus, both activated perivascular and parenchymal astrocytes surrounding inflammatory lesions appear to restrict homing and spread of CD4 T cells to and within the CNS. Mutually not exclusive, the elevated and sustained production of proinflammatory mediators in the spinal cord of GFAP-Cre gp130$^{fl/fl}$ mice (Fig. 5) may contribute to the increased recruitment of autoimmune CD4 T cells and may induce a self-amplificating loop sustaining ongoing inflammation and demyelination. Interestingly, reactive astrocytes also restrict leukocyte infiltration, demyelination, tissue destruction, and motor deficits after traumatic spinal cord injury (43), which further argues for an immunosuppressive function of astrogliosis. However, astrogliosis may not always be protective, because reactive astrocytes inhibit axonal regeneration after spinal cord injury (44) and may prevent oligodendrocyte invasion into demyelinated areas in EAE (7).

In good agreement with Trajkovic et al. (12), who showed that astrocytes can induce regulatory T cell mitigating EAE, we observed that astrocyte loss in GFAP-Cre gp130$^{fl/fl}$ mice did not only result in an increase of activated CD25^{+}CD4 T cells, but also in a decrease of Foxp3^{+} regulatory CD4 T cells. Because regulatory CD4 T cells play an important protective role in EAE (45), their decline in GFAP-Cre gp130$^{fl/fl}$ mice most likely directly contributes to the more severe course of EAE. These phenotypic changes were associated with a significant increase of IL-17–, IFN-γ–, and TNF-producing CD4 T cells in GFAP-Cre gp130$^{fl/fl}$ mice. This increase clearly exceeded the absolute increase of CD4 T cell number in GFAP-Cre gp130$^{fl/fl}$ mice as compared with control animals, which indicates that gp130 signaling in astrocytes is important to shift the balance between protective and EAE-inducing CD4 T cells toward protective T cells. Interestingly, previous in vitro data also provided evidence that astrocytes induce a regulatory phenotype in autoimmune CD4 T cells (12). In addition, CD8 T cells of GFAP-Cre gp130$^{fl/fl}$ mice produced more IFN-γ and TNF. Thus, although gp130-dependent astrocyte loss did not affect the absolute number of CD8 T cells, their proinflammatory cytokine production was increased.

Quantitative RT-PCR revealed that transcription of IL-17, IFN-γ, IL-23, and TNF mRNA was also increased in the CNS of GFAP-Cre gp130$^{fl/fl}$ mice suffering from EAE. IL-17 (46) and IL-23 (47) are key cytokines contributing to EAE. Although IFN-γ is not strictly required for the induction of EAE (48), the ongoing elevated IFN-γ production in GFAP-Cre gp130$^{fl/fl}$ mice may induce the sustained production of iNOS, which can also significantly contribute to development and severity of EAE (49). Thus, the increased Th1/Th17 response combined with an increased transcription of iNOS and IL-23 mRNA by CNS parenchymal cells is likely to account for the more widespread and ongoing demyelination in the absence of astrogliosis in GFAP-Cre gp130$^{fl/fl}$ mice. Noteworthily, transcription of TNF and IL-27 was not elevated and TGF-β2 was even reduced in GFAP-Cre gp130$^{fl/fl}$ mice. This may be explained by the loss of astrocytes in these animals, because astrocytes are a source of these cytokines in EAE (11, 50, 51). Obviously, IL-27 and TGF-β2 transcription by other cells than astrocytes was too low to compensate for loss of astrocyte-derived IL-27 and TGF-β2 and to suppress immunopathology induced by autoimmune T cells, as has been reported before (16, 52).

In this study, we extended our previous genetic approach to dissect the contribution of the two major intracellular signaling cascades engaged by gp130 by creating compound mutant mice that are heterozygous for the corresponding gp130 signaling mutant alleles. These alleles become functionally dominant in astrocytes upon GFAP-Cre–mediated tissue-specific ablation of the paired, conditional *gp130^{fl}* WT allele. Diminished activation of the gp130-SHP2/Ras/ERK pathway in GFAP-Cre gp130$^{fl/Y757F}$ mice reproduced all pathological features observed in gp130 signaling-deficient GFAP-Cre gp130$^{fl/fl}$ mice, including astrocyte loss, lack of astrogliosis, a significantly more severe clinical course, increased T cell infiltration, and severe demyelination. Noteworthily, mice lacking gp130-SHP2/Ras/ERK signaling in all cells may develop spontaneous autoimmune arthritis due to excessive activation of the STAT1/3 pathway in nonhematopoietic cells (53). Although in our model GFAP-Cre gp130$^{fl/Y757F}$ mice with excessive activation of STAT in astrocytes, that is, a nonhematopoietic cell type, showed an exaggerated course of EAE and astrocyte apoptosis, the augmented autoimmune reaction was largely independent of astrocytic gp130-STAT1/3 signaling, because gp130 signaling-deficient GFAP-Cre gp130$^{fl/fl}$ mice reproduced all features of GFAP-Cre gp130$^{fl/Y757F}$ mice. In sharp contrast, GFAP-Cre gp130$^{fl/\Delta STAT}$ mice with intact gp130-SHP2/Ras/ERK signaling developed remarkably milder clinical symptoms as compared with GFAP-Cre gp130$^{fl/Y757F}$ and GFAP-Cre gp130$^{fl/fl}$ mice due to an astrocyte-dependent reduction of autoimmune T cells in the CNS. Noteworthily, our genetic approach in GFAP-Cre gp130$^{fl/\Delta STAT}$ mice is designed to leave STAT1/3 activation by gp130-independent pathways, including the epidermal growth factor and IL-10 signaling, intact. Because STAT3 can be activated by various signaling pathways (reviewed in Ref. 54), STAT3-dependent astrogliosis after spinal cord injury (55) may be caused by the cumulative defective signaling of various pathways and explains why GFAP-Cre gp130$^{fl/\Delta STAT}$ mice still develop astrogliosis in our model. Interestingly, apoptosis of astrocytes in EAE was suppressed by gp130-mediated activation of the SHP2/Ras/ERK pathway and not that of STAT1/3 despite the observation that excessive STAT3 activation provides an antiapoptotic signal in many other cell types (56). In contrast, both astrogliosis and LIF-mediated cardiomyocyte hypertrophy are dependent on the gp130-SHP2/Ras/ERK signaling pathway (57). Collectively, this points to cell-type– and disease-specific functions of these two signaling pathways and establishes astrocytes as an important regulator of cerebral autoimmune reactions.

Acknowledgments

The expert technical assistance of Annette Sohnekind, Nadja Schlüter, and Elena Fischer and the help of Dr. Roland Hartig with cell sorting are gratefully acknowledged. We thank Drs. Ari Waisman (University of Mainz, Mainz, Germany) and Burkard Becher (University of Zürich, Zürich, Switzerland) for critical reading of the manuscript and helpful discussion and Dr. Christoph Köhler (Institute II for Anatomy, University of Cologne, Cologne, Germany) for help with stereology.

Disclosures

The authors have no financial conflicts of interest.

References

1. Tani, M., A. R. Glabinski, V. K. Tuohy, M. H. Stoler, M. L. Estes, and R. M. Ransohoff. 1996. In situ hybridization analysis of glial fibrillary acidic protein mRNA reveals evidence of biphasic astrocyte activation during acute experimental autoimmune encephalomyelitis. *Am. J. Pathol.* 148: 889–896.
2. Brambilla, R., T. Persaud, X. Hu, S. Karmally, V. I. Shestopalov, G. Dvoriantchikova, D. Ivanov, L. Nathanson, S. R. Barnum, and J. R. Bethea. 2009. Transgenic inhibition of astroglial NF-kappa B improves functional outcome in experimental autoimmune encephalomyelitis by suppressing chronic central nervous system inflammation. *J. Immunol.* 182: 2628–2640.
3. van Loo, G., R. De Lorenzi, H. Schmidt, M. Huth, A. Mildner, M. Schmidt-Supprian, H. Lassmann, M. R. Prinz, and M. Pasparakis. 2006. Inhibition of transcription factor NF-kappaB in the central nervous system ameliorates autoimmune encephalomyelitis in mice. *Nat. Immunol.* 7: 954–961.
4. Kang, Z., C. Z. Altuntas, M. F. Gulen, C. Liu, N. Giltiay, H. Qin, L. Liu, W. Qian, R. M. Ransohoff, C. Bergmann, et al. 2010. Astrocyte-restricted ablation of interleukin-17-induced Act1-mediated signaling ameliorates autoimmune encephalomyelitis. *Immunity* 32: 414–425.
5. Qian, Y., C. Liu, J. Hartupee, C. Z. Altuntas, M. F. Gulen, D. Jane-Wit, J. Xiao, Y. Lu, N. Giltiay, J. Liu, et al. 2007. The adaptor Act1 is required for interleukin 17-dependent signaling associated with autoimmune and inflammatory disease. *Nat. Immunol.* 8: 247–256.
6. Hardin-Pouzet, H., M. Krakowski, L. Bourbonnière, M. Didier-Bazes, E. Tran, and T. Owens. 1997. Glutamate metabolism is down-regulated in astrocytes during experimental allergic encephalomyelitis. *Glia* 20: 79–85.
7. Bannerman, P., A. Hahn, A. Soulika, V. Gallo, and D. Pleasure. 2007. Astrogliosis in EAE spinal cord: derivation from radial glia, and relationships to oligodendroglia. *Glia* 55: 57–64.
8. Nair, A., T. J. Frederick, and S. D. Miller. 2008. Astrocytes in multiple sclerosis: a product of their environment. *Cell. Mol. Life Sci.* 65: 2702–2720.
9. Kohji, T., and Y. Matsumoto. 2000. Coexpression of Fas/FasL and Bax on brain and infiltrating T cells in the central nervous system is closely associated with apoptotic cell death during autoimmune encephalomyelitis. *J. Neuroimmunol.* 106: 165–171.
10. Voskuhl, R. R., R. S. Peterson, B. Song, Y. Ao, L. B. Morales, S. Tiwari-Woodruff, and M. V. Sofroniew. 2009. Reactive astrocytes form scar-like perivascular barriers to leukocytes during adaptive immune inflammation of the CNS. *J. Neurosci.* 29: 11511–11522.
11. Fitzgerald, D. C., B. Ciric, T. Touil, H. Harle, J. Grammatikopolou, J. Das Sarma, B. Gran, G. X. Zhang, and A. Rostami. 2007. Suppressive effect of IL-27 on encephalitogenic Th17 cells and the effector phase of experimental autoimmune encephalomyelitis. *J. Immunol.* 179: 3268–3275.
12. Trajkovic, V., O. Vuckovic, S. Stosic-Grujicic, D. Miljkovic, D. Popadic, M. Markovic, V. Bumbasirevic, A. Backovic, I. Cvetkovic, L. Harhaji, et al. 2004. Astrocyte-induced regulatory T cells mitigate CNS autoimmunity. *Glia* 47: 168–179.
13. Gimsa, U., A. ØRen, P. Pandiyan, D. Teichmann, I. Bechmann, R. Nitsch, and M. C. Brunner-Weinzierl. 2004. Astrocytes protect the CNS: antigen-specific T helper cell responses are inhibited by astrocyte-induced upregulation of CTLA-4 (CD152). *J. Mol. Med.* 82: 364–372.
14. Sofroniew, M. V., and H. V. Vinters. 2010. Astrocytes: biology and pathology. *Acta Neuropathol.* 119: 7–35.
15. Ernst, M., and B. J. Jenkins. 2004. Acquiring signalling specificity from the cytokine receptor gp130. *Trends Genet.* 20: 23–32.
16. Batten, M., J. Li, S. Yi, N. M. Kljavin, D. M. Danilenko, S. Lucas, J. Lee, F. J. de Sauvage, and N. Ghilardi. 2006. Interleukin 27 limits autoimmune encephalomyelitis by suppressing the development of interleukin 17-producing T cells. *Nat. Immunol.* 7: 929–936.
17. Eugster, H. P., K. Frei, M. Kopf, H. Lassmann, and A. Fontana. 1998. IL-6-deficient mice resist myelin oligodendrocyte glycoprotein-induced autoimmune encephalomyelitis. *Eur. J. Immunol.* 28: 2178–2187.
18. Linker, R. A., M. Mäurer, S. Gaupp, R. Martini, B. Holtmann, R. Giess, P. Rieckmann, H. Lassmann, K. V. Toyka, M. Sendtner, and R. Gold. 2002. CNTF is a major protective factor in demyelinating CNS disease: a neurotrophic cytokine as modulator in neuroinflammation. *Nat. Med.* 8: 620–624.
19. Butzkueven, H., J. G. Zhang, M. Soilu-Hanninen, H. Hochrein, F. Chionh, K. A. Shipham, B. Emery, A. M. Turnley, S. Petratos, M. Ernst, et al. 2002. LIF receptor signaling limits immune-mediated demyelination by enhancing oligodendrocyte survival. *Nat. Med.* 8: 613–619.
20. Stahl, N., T. J. Farruggella, T. G. Boulton, Z. Zhong, J. E. Darnell, Jr., and G. D. Yancopoulos. 1995. Choice of STATs and other substrates specified by modular tyrosine-based motifs in cytokine receptors. *Science* 267: 1349–1353.
21. Tebbutt, N. C., A. S. Giraud, M. Inglese, B. Jenkins, P. Waring, F. J. Clay, S. Malki, B. M. Alderman, D. Grail, F. Hollande, et al. 2002. Reciprocal regulation of gastrointestinal homeostasis by SHP2 and STAT-mediated trefoil gene activation in gp130 mutant mice. *Nat. Med.* 8: 1089–1097.
22. Ohtani, T., K. Ishihara, T. Atsumi, K. Nishida, Y. Kaneko, T. Miyata, S. Itoh, M. Narimatsu, H. Maeda, T. Fukada, et al. 2000. Dissection of signaling cascades through gp130 in vivo: reciprocal roles for STAT3- and SHP2-mediated signals in immune responses. *Immunity* 12: 95–105.
23. Bajenaru, M. L., Y. Zhu, N. M. Hedrick, J. Donahoe, L. F. Parada, and D. H. Gutmann. 2002. Astrocyte-specific inactivation of the neurofibromatosis 1 gene (NF1) is insufficient for astrocytoma formation. *Mol. Cell. Biol.* 22: 5100–5113.
24. Betz, U. A., W. Bloch, M. van den Broek, K. Yoshida, T. Taga, T. Kishimoto, K. Addicks, K. Rajewsky, and W. Müller. 1998. Postnatally induced inactivation of gp130 in mice results in neurological, cardiac, hematopoietic, immunological, hepatic, and pulmonary defects. *J. Exp. Med.* 188: 1955–1965.
25. Zhu, Y., M. I. Romero, P. Ghosh, Z. Ye, P. Charnay, E. J. Rushing, J. D. Marth, and L. F. Parada. 2001. Ablation of NF1 function in neurons induces abnormal development of cerebral cortex and reactive gliosis in the brain. *Genes Dev.* 15: 859–876.
26. Steinbrecher, A., D. Reinhold, L. Quigley, A. Gado, N. Tresser, L. Izikson, I. Born, J. Faust, K. Neubert, R. Martin, et al. 2001. Targeting dipeptidyl peptidase IV (CD26) suppresses autoimmune encephalomyelitis and up-regulates TGF-beta 1 secretion in vivo. *J. Immunol.* 166: 2041–2048.
27. Schlüter, D., J. Löhler, M. Deckert, H. Hof, and G. Schwendemann. 1991. *Toxoplasma* encephalitis of immunocompetent and nude mice: immunohistochemical characterisation of *Toxoplasma* antigen, infiltrates and major histocompatibility complex gene products. *J. Neuroimmunol.* 31: 185–198.
28. Rosen, G. D., and J. D. Harry. 1990. Brain volume estimation from serial section measurements: a comparison of methodologies. *J. Neurosci. Methods* 35: 115–124.
29. Schlüter, D., S. B. Oprisiu, S. Chahoud, D. Weiner, O. D. Wiestler, H. Hof, and M. Deckert-Schlüter. 1995. Systemic immunization induces protective CD4+ and CD8+ T cell-mediated immune responses in murine *Listeria monocytogenes* meningoencephalitis. *Eur. J. Immunol.* 25: 2384–2391.
30. Livak, K. J., and T. D. Schmittgen. 2001. Analysis of relative gene expression data using real-time quantitative PCR and the 2(-Δ Δ C(T)) method. *Methods* 25: 402–408.
31. Drögemüller, K., U. Helmuth, A. Brunn, M. Sakowicz-Burkiewicz, D. H. Gutmann, W. Mueller, M. Deckert, and D. Schlüter. 2008. Astrocyte gp130 expression is critical for the control of *Toxoplasma* encephalitis. *J. Immunol.* 181: 2683–2693.
32. Pender, M. P., and M. J. Rist. 2001. Apoptosis of inflammatory cells in immune control of the nervous system: role of glia. *Glia* 36: 137–144.
33. Klein, C., T. Wüstefeld, U. Assmus, T. Roskams, S. Rose-John, M. Müller, M. P. Manns, M. Ernst, and C. Trautwein. 2005. The IL-6-gp130-STAT3 pathway in hepatocytes triggers liver protection in T cell-mediated liver injury. *J. Clin. Invest.* 115: 860–869.
34. Linker, R. A., N. Kruse, S. Israel, T. Wei, S. Seubert, A. Hombach, B. Holtmann, F. Luhder, R. M. Ransohoff, M. Sendtner, and R. Gold. 2008. Leukemia inhibitory factor deficiency modulates the immune response and limits autoimmune demyelination: a new role for neurotrophic cytokines in neuroinflammation. *J. Immunol.* 180: 2204–2213.
35. Streetz, K. L., T. Wüstefeld, C. Klein, K. J. Kallen, F. Tronche, U. A. Betz, G. Schütz, M. P. Manns, W. Müller, and C. Trautwein. 2003. Lack of gp130 expression in hepatocytes promotes liver injury. *Gastroenterology* 125: 532–543.
36. Renno, T., M. Krakowski, C. Piccirillo, J. Y. Lin, and T. Owens. 1995. TNF-alpha expression by resident microglia and infiltrating leukocytes in the central nervous system of mice with experimental allergic encephalomyelitis: regulation by Th1 cytokines. *J. Immunol.* 154: 944–953.
37. Ozawa, K., G. Suchanek, H. Breitschopf, W. Brück, H. Budka, K. Jellinger, and H. Lassmann. 1994. Patterns of oligodendroglia pathology in multiple sclerosis. *Brain* 117: 1311–1322.
38. Ransohoff, R. M., T. A. Hamilton, M. Tani, M. H. Stoler, H. E. Shick, J. A. Major, M. L. Estes, D. M. Thomas, and V. K. Tuohy. 1993. Astrocyte expression of mRNA encoding cytokines IP-10 and JE/MCP-1 in experimental autoimmune encephalomyelitis. *FASEB J.* 7: 592–600.
39. Pender, M. P., K. B. Nguyen, P. A. McCombe, and J. F. Kerr. 1991. Apoptosis in the nervous system in experimental allergic encephalomyelitis. *J. Neurol. Sci.* 104: 81–87.
40. Schmied, M., H. Breitschopf, R. Gold, H. Zischler, G. Rothe, H. Wekerle, and H. Lassmann. 1993. Apoptosis of T lymphocytes in experimental autoimmune encephalomyelitis: evidence for programmed cell death as a mechanism to control inflammation in the brain. *Am. J. Pathol.* 143: 446–452.
41. Bonetti, B., J. Pohl, Y. L. Gao, and C. S. Raine. 1997. Cell death during autoimmune demyelination: effector but not target cells are eliminated by apoptosis. *J. Immunol.* 159: 5733–5741.
42. Bechmann, I., B. Steiner, U. Gimsa, G. Mor, S. Wolf, M. Beyer, R. Nitsch, and F. Zipp. 2002. Astrocyte-induced T cell elimination is CD95 ligand dependent. *J. Neuroimmunol.* 132: 60–65.
43. Faulkner, J. R., J. E. Herrmann, M. J. Woo, K. E. Tansey, N. B. Doan, and M. V. Sofroniew. 2004. Reactive astrocytes protect tissue and preserve function after spinal cord injury. *J. Neurosci.* 24: 2143–2155.
44. Menet, V., M. Prieto, A. Privat, and M. Giménez y Ribotta. 2003. Axonal plasticity and functional recovery after spinal cord injury in mice deficient in both glial fibrillary acidic protein and vimentin genes. *Proc. Natl. Acad. Sci. USA* 100: 8999–9004.
45. McGeachy, M. J., L. A. Stephens, and S. M. Anderton. 2005. Natural recovery and protection from autoimmune encephalomyelitis: contribution of CD4+CD25+ regulatory cells within the central nervous system. *J. Immunol.* 175: 3025–3032.
46. Komiyama, Y., S. Nakae, T. Matsuki, A. Nambu, H. Ishigame, S. Kakuta, K. Sudo, and Y. Iwakura. 2006. IL-17 plays an important role in the development of experimental autoimmune encephalomyelitis. *J. Immunol.* 177: 566–573.
47. Becher, B., B. G. Durell, and R. J. Noelle. 2003. IL-23 produced by CNS-resident cells controls T cell encephalitogenicity during the effector phase of experimental autoimmune encephalomyelitis. *J. Clin. Invest.* 112: 1186–1191.
48. Ferber, I. A., S. Brocke, C. Taylor-Edwards, W. Ridgway, C. Dinisco, L. Steinman, D. Dalton, and C. G. Fathman. 1996. Mice with a disrupted IFN-gamma gene are susceptible to the induction of experimental autoimmune encephalomyelitis (EAE). *J. Immunol.* 156: 5–7.

49. Fenyk-Melody, J. E., A. E. Garrison, S. R. Brunnert, J. R. Weidner, F. Shen, B. A. Shelton, and J. S. Mudgett. 1998. Experimental autoimmune encephalomyelitis is exacerbated in mice lacking the NOS2 gene. *J. Immunol.* 160: 2940–2946.
50. Siglienti, I., A. Chan, C. Kleinschnitz, S. Jander, K. V. Toyka, R. Gold, and G. Stoll. 2007. Downregulation of transforming growth factor-beta2 facilitates inflammation in the central nervous system by reciprocal astrocyte/microglia interactions. *J. Neuropathol. Exp. Neurol.* 66: 47–56.
51. Sun, D., C. Coleclough, L. Cao, X. Hu, S. Sun, and J. N. Whitaker. 1998. Reciprocal stimulation between TNF-alpha and nitric oxide may exacerbate CNS inflammation in experimental autoimmune encephalomyelitis. *J. Neuroimmunol.* 89: 122–130.
52. Faunce, D. E., A. Terajewicz, and J. Stein-Streilein. 2004. Cutting edge: in vitro-generated tolerogenic APC induce CD8+ T regulatory cells that can suppress ongoing experimental autoimmune encephalomyelitis. *J. Immunol.* 172: 1991–1995.
53. Atsumi, T., K. Ishihara, D. Kamimura, H. Ikushima, T. Ohtani, S. Hirota, H. Kobayashi, S. J. Park, Y. Saeki, Y. Kitamura, and T. Hirano. 2002. A point mutation of Tyr-759 in interleukin 6 family cytokine receptor subunit gp130 causes autoimmune arthritis. *J. Exp. Med.* 196: 979–990.
54. Aggarwal, B. B., G. Sethi, K. S. Ahn, S. K. Sandur, M. K. Pandey, A. B. Kunnumakkara, B. Sung, and H. Ichikawa. 2006. Targeting signal-transducer-and-activator-of-transcription-3 for prevention and therapy of cancer: modern target but ancient solution. *Ann. N. Y. Acad. Sci.* 1091: 151–169.
55. Herrmann, J. E., T. Imura, B. Song, J. Qi, Y. Ao, T. K. Nguyen, R. A. Korsak, K. Takeda, S. Akira, and M. V. Sofroniew. 2008. STAT3 is a critical regulator of astrogliosis and scar formation after spinal cord injury. *J. Neurosci.* 28: 7231–7243.
56. Bromberg, J., and J. E. Darnell, Jr. 2000. The role of STATs in transcriptional control and their impact on cellular function. *Oncogene* 19: 2468–2473.
57. Nakaoka, Y., K. Nishida, Y. Fujio, M. Izumi, K. Terai, Y. Oshima, S. Sugiyama, S. Matsuda, S. Koyasu, K. Yamauchi-Takihara, et al. 2003. Activation of gp130 transduces hypertrophic signal through interaction of scaffolding/docking protein Gab1 with tyrosine phosphatase SHP2 in cardiomyocytes. *Circ. Res.* 93: 221–229.